2024 7th International Conference on Soft Robotics (RoboSoft)
San Diego, CA, USA. April 14-17, 2024

Modular and Reconfigurable Body Mounted Soft Robots

Tuo Liu, Taqi Abrar, and Jonathan Realmuto

***Abstract*— Movement disorders reduce muscle strength and mobility, and while therapeutic interventions aim to maintain mobility, many individuals with impairments are unable to function independently. Soft wearable robots (exosuits) are envisioned to provide long-term daily physical assistance to the mobility impaired, however, there is still no such commercial device widely available. A main challenge is the design, fabrication, and mounting of soft actuators to the human body. Here, we describe a canonical design framework for the development of soft, modular, and reconfigurable pneumatically driven soft actuators manufactured using textiles. Through the use of an innovative 3D-printed self-sealing end-cap, our method provides a simple and effective way for uniting and hermetically sealing actuators constructed through a layered fabrication process, where a (mechanically programmable) textile sleeve surrounds an internal bladder. To mount the actuators to the body, we have developed a semi-rigid interface consisting of modular segments that fasten together to form cylindrical units that can be mounted to the limb and include snap-in fasteners to attach actuators. The human-robot interfaces act to secure the actuators to the body and to optimize and distribute mechanical power transfer over a large area. Taken together, our proposed modular architecture allows the actuators and their attachment points to be easily modified so that an exosuit for the knee, elbow, or other joints, can be realized with the same set of hardware. We demonstrated our proposed design on a realistic human leg mannequin and our results verify its ability to provide substantial force to the body.**

I. Introduction

Movement disorders, including Parkinson's disease, tremor, and dystonia, are common conditions that affect one's ability to move volitionally, often impacting independence. Some movement disorders are a results of abnormal brain development or damage to the developing brain, for example, cerebral palsy, which is the most common cause of serious physical disability in childhood [1], while others have a genetic basis, such as nemaline myopathy, a rare group of diseases affecting skeletal muscle [2]. In most cases, there are no curative treatments and exercise and physiotherapy are the main therapeutic methods aimed at maintaining muscle strength and mobility [3], [4]. Assistive devices like wearable robots are envisioned for daily, ongoing physical support, and thus could play a significant role in treatments [5]. Recent innovations in soft robotics are enabling a new generation of lightweight, compliant, and safe wearable robots, e.g., exosuits [6]–[8]. However, in most cases, these devices are designed on an ad-hoc basis, and there has not yet emerged a clear methodology for designing and fabricating exosuits for general assistive applications.

*This research was support by *A Foundation Building Strength*.

Tuo Liu, Taqi Abrar, and Jonathan Realmuto are with the Bionic Systems Lab, Department of Mechanical Engineering, University of California, Riverside, 900 University Ave. Riverside, CA 92521. (tliu189, taqia, jonathan.realmuto)@ucr.edu

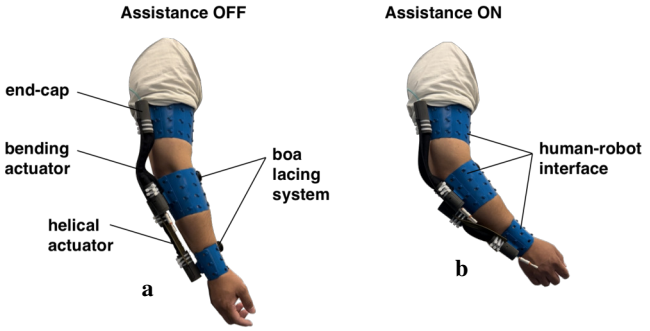

Fig. 1. A two-degree-of-freedom exosuit fabricated using our method that provides torques in elbow flexion and forearm supination. **a** Exosuit with assistance off, and **b** exosuit with assistance on. The major components are labeled and consist of the end-cap, actuators (a bending actuator for elbow flexion, and an helical actuator for forearm supination), the human-robot interface, and the BOA lacing systems used to tighten the interface onto the limb.

During physical human-robot interactions with assistive robots, bulky and rigid devices limit the natural workspace of limbs, are prone to kinematic incompatibilities [9], and require compensatory nonphysiological muscle strategies due to added inertia [10]. Therefore, there is a need for a lightweight, easy-to-fit device that is compliant with the human body. Using soft structures can minimize or eliminate the need for bulky and heavy robots [11], which have traditionally been the standard for rehabilitative applications [12]. Apart from providing safety to the user, soft devices can provide high power-to-torque ratio, compliance with the human body, and low fabrication costs [13]. However, there exists multiple classes of soft robotic actuators, including fluidic [14], tendon-driven [15], pneumatic [16], [17] or a combination [18], and no single strategy has as emerged as the dominate technology.

Soft textile-based pneumatic actuators are an emerging technology with desirable characteristics in the context of wearable robots, including their lightweight, compliance, and inherent safety. These actuators leverage deformations in the body of the actuator to create motion by exploiting anisotropic mechanical responses in the textiles [19]. Depending on the choice of textiles used, their orientations, and how they are joined, many different motion modalities are possible, including bending, twisting, and rigidizing [20]–[22]. Such actuators have been incorporated into exosuits for the shoulder [23], [24], hand [25], knee [26], ankle [27], and forearm [28]. However, most of the these designs vary radically, each with a different fabrication technique and body mounting procedure.

This paper presents a fabrication method for modular, reconfigurable, light-weight, and low-cost soft exosuits. The

2024 IEEE 7th International Conference on Soft Robotics (RoboSoft) | 979-8-3503-8181-8/24/$31.00 ©2024 IEEE | DOI: 10.1109/ROBOSOFT60065.2024.10521986

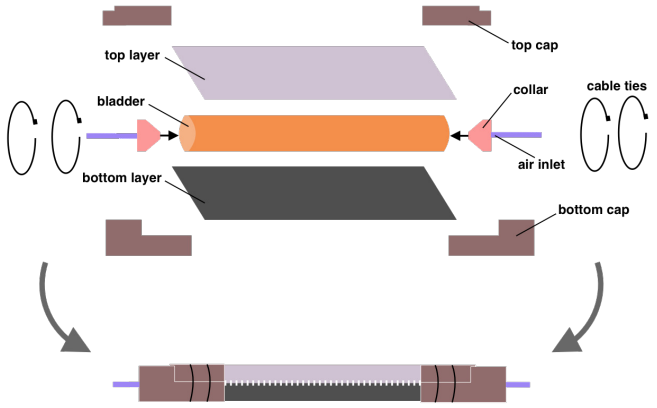

Fig. 2. Exploded view (top) and final actuator (bottom) illustrating the universal fabrication technique. Two fabric layers encase a extensible bladder. The bladder has collars with air inlets tubes inserted on both end. The fabrics are sewing together (not shown) and the top and bottom end-caps unity the individual components. As a last step cable ties are used to secure the end-caps (not shown).

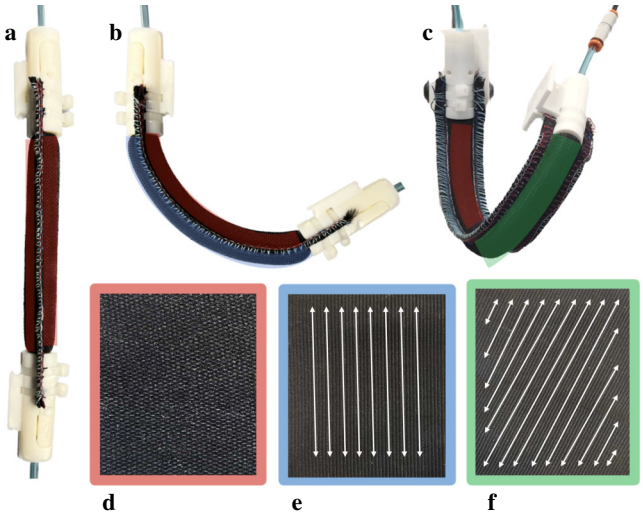

Fig. 3. Summary of three possible motion modalities for the soft actuators. Rigidizing (**a**), bending (**b**), and helical (**c**) actuators. Here, the top layer fabric choice determines the motion modality. All actuators have an inelastic bottom layer (**d**) and the rigidizing actuator also uses an inelastic bottom layer, the bending actuator uses a knit elastic top layer with the stretch oriented longitudinally (**e**), while the helical actuator uses a knit elastic top layer with the alignment off axis (**f**).

exosuits leverage textile-based pneumatic actuators, which can be realized for a variety of motions, together with a modular human-robot interface to secure the actuators to the body. A prototype exosuit, fabricated using our method, is shown in Fig. 1 and consists of two actuators, one for elbow flexion and one for forearm supination, and three modular human-robot interfaces used to secure the actuators to the body. At the center of our method is a self sealing end-cap that simplifies actuator assembly. The actuator sleeves, which determine the motion modality, are all fabricated using identical procedures, with the only difference being the choice of textile material and orientation to determine the motion modality. In this way, we have developed a streamlined fabrication procedure for a large class of motions. To physically attached the actuators to the body, we have designed a modular human-robot interface that consists of segmented semi-rigid plates that are joined together to form a cylindrical shape to conform to the limbs. The size of the cylindrical interface is easily changed by adding or subtracting segments and the interface is secured to the limb using a BOA lacing system. The actuators snap-in to the interfaces via specialized structures 3D-printed on the end-cap and interfaces, making the whole system modular and reconfigurable.

II. Fabrication Framework

A. Problem statement and assembly overview

While soft robots have traditionally relied on a variety of fabrication techniques to create the actuator body, including casting, injection molding, 3D printing, fabrics, and others [29]–[34], one general approach is to use an internal bladder with a functional outer sleeve, e.g., the traditional McKibben pneumatic artificial muscle [35]. In this configuration, when the internal bladder is pressurized, the bladder surfaces expands and pushes against the sleeve. The sleeve architecture is what determines the resulting motion, and, in practice, is mechanically programmed to selectively expand in certain regions. Hose fittings and metal clamps are typically used to seal the bladder and to secure the sleeve onto the bladder. However, there are number of drawbacks in this configuration. The clamps can cut into the softer bladder material, leading to concealed damage around the sealing edge, and compromising the system's integrity by reducing the holding pressure, and leaving the potential for air leaks. Another issue is mounting the actuators to the body. With the hose fitting and clamp configuration, there is no dedicated way to mechanical attached the actuator, and so improvised straps are typically used to fasten the actuator to the body. We aim to solve the problems of sealing/uniting the actuator components and securely attaching the actuators onto human limbs in a modular way that allows for easy reconfiguration.

In our proposed framework, all actuator modalities leverage an identical fabrication procedure, outlined in Fig. 2. The layered-based fabrication has four key component for the actuator. The air inlet, it allows air to flow in and out, and composed of two distinct components: the inner collar and the inlet tube. The next component is the bladder which can be made of silicon or latex. The third component is the fabric sleeve, programmed to restrict bladder expansion in certain directions. The last one is end-cap, it merges the sleeve and bladder into one single entity, it has one top piece and one bottom piece. In practice, the sleeve can be programmed for a variety of different motions, however, in this work we restrict the motions to following, which are summarized in Fig. 3, rigidizing: composed with inelastic fabric on the top and bottom layers; bending: made with inelastic fabric on the bottom layer and knit elastic fabric on the top layer with the stretch directions oriented longitudinally; and helical: made with inelastic fabric on the bottom layer and knit elastic fabric on the top layer with the stretch directions oriented

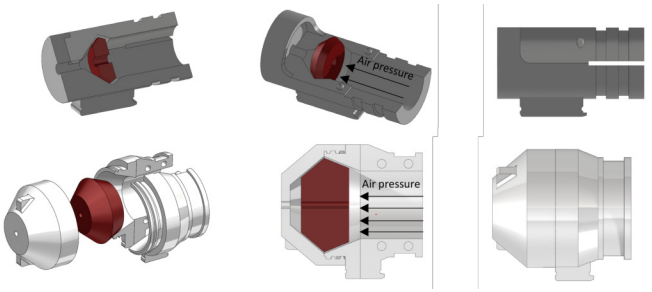

Fig. 4. 3D renders of the self-sealing end-caps. Top row: two element end-cap, designed for smaller bladders. Bottom row: three element end-cap for larger bladders. Each design incorporates the self-sealing collar which is inserted into the bladder. The internal pressure of the actuator ensures a hermetic seal. The two element end-cap (top row) features a clip and press design, where the top cap and bottom cap compresses together. The three element end-cap (bottom row) features a continuously thread dome with two body pieces.

off axis (the axis angle determines the helical shape [28]).

B. Self-sealing end-cap

We have designed two different end-caps, shown in Fig. 4, that prevent air leaks, and combine and seal all components of the actuator into a unit. The first design works best for smaller actuators (bladder radius $<$ 12 mm) and is constructed from two independent elements. The other is designed for bigger actuators and constructed from three independent elements. Both designs leverage the same self sealing principle. While the initial two element design emphasized simplicity and works well for smaller actuators, it can damage the thin-walled and soft bladders that are typically used with larger actuators. The three element end-cap solves this issue and offers improved sealing, but requires a more accurate 3D printer for fabrication. The two element end-cap is designed to utilize a clip and push mechanism and eliminates the need for accurate and precise 3D printing. The three element end-cap is more intricate and consist of left and right pieces that clip together to hold the bladder and sleeve, and a top continuously thread dome, which is thread to the other two elements to complete the seal.

The working Principle of the end-caps are to use the internal bladder pressure to generate a sealing force to prevent leaking, and is achieved via the inner bladder collar (red), as shown in Fig. 4. The gap between the inner collars are engineered to be half the thickness of the bladder. When the top and bottom housings are fastened together, this configuration deforms the bladder, effectuating the initial sealing. For the two element design, the end-caps have mortise and tenon joints, and by utilizing the principle of leverage, only a small amount of force is required to fastened the top and bottom caps. As we clamp the bladder, the bladder is fasten and locked in all directions, at the same time, it will have even pressure around the edge of inner collar, so it will not cause any damage. The three element design seals similiarly with a continuous thread. When the actuator is pressurized, the internal air pressure will create force on inner collar, push it against the wall of end-cap, create a second stage of sealing.

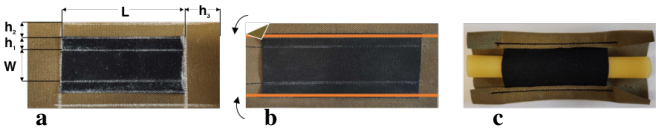

Fig. 5. Details of the sleeve fabrication process. **a** The pattern is cut and chalked to mark the sewing lines (seams). **b** The two layers are sewn together, then the top layer is folded over the bottom layer. **c** After the final seam is sewn, the bladder can be inserted to ensure a good fit. The extra material at either end is trimmed before the end-caps are installed.

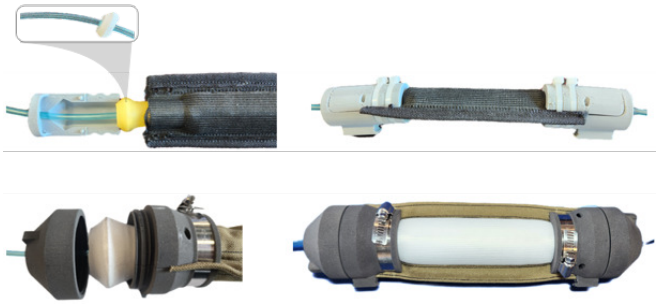

Fig. 6. Two prototype actuators showing details for the sleeve and end-cap assembly. Inset shows bladder collar and inlet details.

C. Sleeve fabrication

The process of fabricating the functional sleeve consists of designing the pattern and sewing together the two layers. The nominal actuator pattern, shown in Fig. 5, should be taken as the length L of the desired actuator, with some extra space allocated at each edge (h_3 in Fig. 5). The width W should equal half the circumference of the bladder, plus a few millimeter of room for movement. Special care is required to ensure space for the seams and in practice we allocated two extra spaces, h_1 (see Fig. 5) provides the first seam spacing, while h_2, which is extra fabric on the bottom layer, allows the bottom to folded over the top fabric for the final seam. For our actuators the seam spacing varies depending on size, but $h_1 = h_2 = 3$ cm, is a good start. First sew the two piece of fabric together along the two edges of the bladder seam. Then fold the bottom fabric over and sew one more time as in Fig. 5**c**. Insert the bladder to ensure a good fit. The bladder should be easy to insert, but not have extra spacing on either side. We use a Singer Heavy Duty (4452) sewing machine with the following settings: tension 4.5, length 2.5, triple stitch for first seam and single stitch after fold.

The behavior of the actuator is strictly associated with its fabric sleeve. The rigidizing actuator is composed using the same two fabric materials, a non-stretch woven fabric (e.g., ballistic nylon (Magna Fabrics, 1050 Denier Coated Ballistic Nylon Fabric)). As depicted in Figure 3 the rigidizing actuator becomes stiff and rigid when inflated, and it neither extends nor contracts during activation. This is because the walls of the bladder push against the sleeve when pressurized, and the non-stretch woven fabric expands outward, resulting in a pneumatic beam. The bending and helical actuators are fabricated in the same way, with the only difference being the substitution of the elastic fabric top layer. We use a knit elastic fabric (Cisone, Heavy Stretch

Fig. 7. Details of the modular human-robot interface. **a** The central segments are used for attaching actuators. **b** The extending segments are used to extend the interface to form the cylindrical structure. **c** The end segment is used to nearly complete the cylinder, ensure the extruded poles are on both of the last two segments. **d** The BOA lace system is fasten to a floating segment, placed under (closest to the skin) the last two segments, with lacing wrapping the extruded poles. Tightening the BOA secures the interface to the limb. **e** Details of the mounting mechanism for the actuators.

High Elasticity Knit Elastic Band), which are commonly found as the waist band in garments, and have anisotropic elastic properties, being highly stretchable in only one dimension. The knit elastic fabric is cut in a way that its stretch directions are parallel to the length for the bending actuators, and off axis for the helical actuators [28], as shown in Fig. 3. Two fabricated actuators are shown in Fig. 6, illustrating the assembly of the sleeve and end-caps for the two different end-cap designs.

D. Modular human-robot interface

To facilitate the attachment to a limb, we have designed a modular human-robot interface consisting of four distinct parts, as shown in Fig. 7, which are interconnected using 3D printed poles and holes, mimicking the interlocking design of lamellar armor plates. The central section, (Fig. 7**a**) allows an actuator to be connected, while the extending segments (Fig. 7**b**) extend the cylindrical form. The end segment (Fig. 7**c**) is used to almost complete the cylinder and ensures that the extruded poles are on both ends of the two segments to be joined. The final segment is floating and positioned directly onto the skin, and has the BOA lacing system (`https://www.boafit.com`), which is then looped over the extruded poles, as shown in Fig. 7**d**. Tightening the BOA secures the interface to the body. Each interface segment is engineered with a thickness ($\approx$ 0.75 mm) that keeps a balance between providing adequate rigidity against the actuator's force and allowing flexibility to conform to limb curvature. With the minor adjustment of top and bottom length of each piece, the combined system has the ability to cover any curvatures of radius, providing a universal interface for most body surface.

The actuators attached to the modular interface via a compression fitting mechanism so that the entire system is easily integrated and reconfigured. This design facilitates the flexibility for users to adapt the actuator configuration based on their specific requirements. The details of the mounting mechanism are shown in Fig. 7**e**. The elongated portion at the bottom of the end-cap ensures a robust connection to the interface. The notches on either side guarantee the end-cap's stable positioning within the interface, while the clip on this extended part serves as a guide during installation. When installing, the clip end is inserted into the interface, followed by pressing down on the notched end. To remove the pneumatic actuators, one simply needs to lift the previously pressed down notch end, enabling the actuator to easily detach from the interface. This design not only offers convenience but also assures a sturdy mount and removal process for the pneumatic actuators. The interface's modularity means actuators can be affixed to various bases in different orientations.

III. Experimental Results

A. Evaluation of the hermetic properties of the end-caps

To validate the effectiveness of the end-caps, we conducted a experimental cyclic evaluation test. In this setup, the actuator was suspended above a table using two aluminum rails for support. A Beaglebone Black single board computer, in conjunction with two solenoid values (SMC, SY113-SMO-PM-F) and a pressure sensor (Honeywell, HSC-SANN150PG2A3), were used to automatically regulate the internal bladder pressure. If the pneumatic actuator failed to maintain its pressure at any point during the test, the procedure would terminate immediately. Throughout this test, the pneumatic actuator was inflated to 620 kPa (90 psi), sustained for 5 seconds, then deflated, repeating this cycle for a continuous 8-hour duration. During the experiment, no leaks were detected. In addition to this, to visualized that the actuator is sealed and will create a leakproof system, the inflated actuator was submerged into a water to check for any signs of air leakage. When the system was fitted with the intended end caps, there were no visible air bubbles after submersion, providing evidence of the hermetic seal.

B. Force generation of the rigidizing and bending actuators

To determine the force generating characteristic of the rigidizing and bending actuators, experiments were conducted using the setups shown in Fig. 8. We fabricated actuators with bladder radii of 6 mm, 9 mm, and 19 mm, and with lengths of 70 mm, 140 mm, 210 mm, and 280 mm. For the bending actuators, the testing configuration was with the actuator fully extended, as shown in Fig. 8**a**. For the rigidizing actuators, the testing configuration was with the actuator bent 90° at the center, as shown in Fig. 8**b**. During each experiment the actuator was pressured use a staircase pressure profile with a range from 0 to 690 kPa (100 psi) in

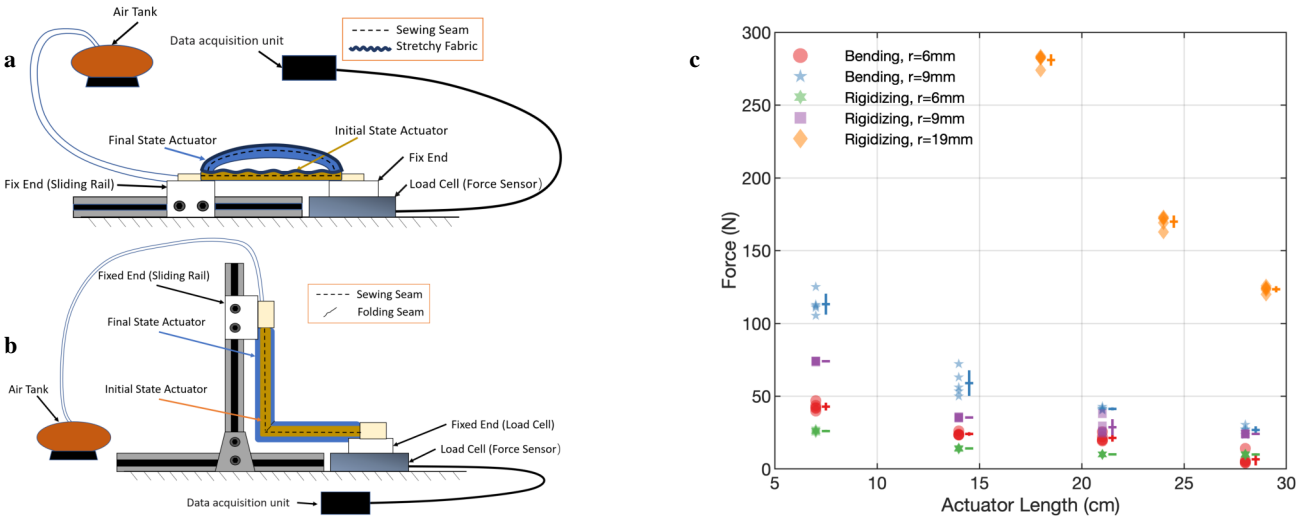

Fig. 8. Experimental setups and results for the block force experiments. **a** Setup for the bending actuator consisting of the actuator secured to the fixture with a load cell measure the force characteristics. **b** The setup for the rigidizing actuators is identical, except for the actuator is configured with a 90° bend at the center. **c** Scatter plot of the force-generating characteristics for rigidizing and bending actuators with varying lengths and radii. Each actuator was tested five times and the mean (horizontal line) and standard deviation (vertical lines) are indicated next to each set of measurements. The trend indicates that larger radius and shorter length results in greater forces.

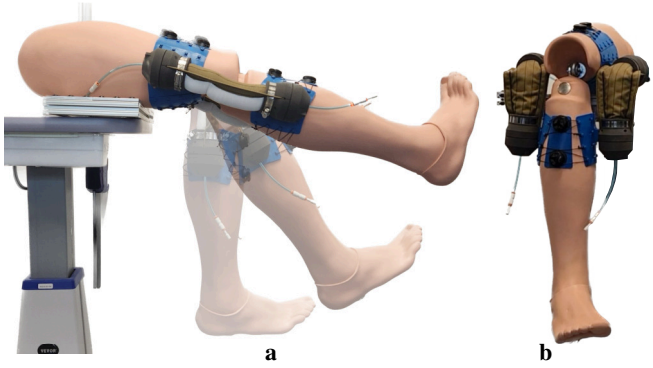

Fig. 9. Demonstration of the prototype knee exosuit lifting a human scale mannequin leg (5 kg). **a** Sequence of superimposed images in the sagittal plane demonstrating leg lifting. Foreground image is at full pressure. **b** Frontal plane view showing both actuators (deflated state).

increments of 34 kPa (5 psi) for each step, which lasted two seconds. A six axis load cell (ATI Industrial Automation, Model Delta) captured the force characteristics during the experiments.

The net actuator force for each experiment was taken as the squared sum of the vertical and in plane forces captured by the load cell. The maximum force for each actuator is shown in Fig. 8**c**, and the results indicate that the bladder radius (and subsequently the fabric sleeve width) plays a critical role in determining the force characteristics. When the radius is increased, the amount of force the actuator exerts increases. Each experiment was conducted five times, and the means and standard deviations included in Fig. 8**c**. The maximum achievable force inversely scales with actuator length. We found that the rigidizing actuator with r = 19 mm and L = 18.8 cm produced a maximum force of greater than 250 N at 690 kPa (100 psi).

The results in Fig. 8**c** demonstrate the scalability of the actuator design. The inner tube of the actuator is readily available commercially in various radius and length configurations. Additionally, the outer sleeve, made from fabric, can be customized to accommodate any desired radius and length. The end caps, essential components for sealing the actuator, can be 3D printed to fit various radii. While the maximum sealing capability of the end caps has not been precisely determined, during experimental testing, no air leakage was observed within the tested pressure range of up to 827 kPa (120 psi), indicating effective performance. However, it is important to note that increasing the radius of the actuator also necessitates an increase in the minimum length of the actuator. For example, in the case of the actuator with a 19 mm radius, a length shorter than 170 mm would prevent the actuator from bending adequately. This limitation occurs as a shorter length would lead to end cap collision, preventing the actuator from bending.

C. Wearable knee exosuit

We developed a knee exosuit, as shown in Fig.9, with two bending actuators for knee flexion. The two actuators are attached either side of the knee, highlighting our interface's modularity. To test the exosuit's torque assistance, we employed a human-sized mannequin (Rescue Randy 145-lb) targeting to lift an adult leg's weight. The mannequin's lower leg weighed about 5 Kg. Secured at the knee, the exosuit lifted the joint smoothly as actuators inflated from 0 to 662 kPa (96 psi), depicted in Fig.9.

IV. Conclusions

We have presented a fabrication framework for modular and reconfigurable soft robotic exosuits. The methodology includes a single canonical fabrication method for tubular soft pneumatically driven actuators that can realize a variety

of motion modalities through mechanically programming the functional sleeve. The actuators are secured to the body via a modular and reconfigurable human-robot interface, which is constructed as a semi-flexible cylindrical unit that can be adjusted to fit any human limb. Whereas exosuits often target single joints like shoulder, knee, elbow, limiting their use to a particular functions, our method can realize a variety of exosuits for a wider range of body applications, all with the same hardware components. We have shown through experimental evaluations our proposed framework can achieve high performance soft actuators, and have shown through two different exosuit applications our method's flexibility, modularity, and reconfigurability.

REFERENCES

[1] C. Morris, "Definition and classification of cerebral palsy: a historical perspective," *Developmental Medicine & Child Neurology*, vol. 49, pp. 3–7, 2007.

[2] C. A. Sewry, J. M. Laitila, and C. Wallgren-Pettersson, "Nemaline myopathies: a current view," *Journal of Muscle Research and Cell Motility*, vol. 40, pp. 111–126, 2019.

[3] A. Adaikina, P. L. Hofman, G. L. O'Grady, and S. Gusso, "Exercise training as part of musculoskeletal management for congenital myopathy: where are we now?" *Pediatric Neurology*, vol. 104, pp. 13–18, 2020.

[4] O. Verschuren, M. Ketelaar, J. W. Gorter, P. J. Helders, C. S. Uiterwaal, and T. Takken, "Exercise training program in children and adolescents with cerebral palsy: a randomized controlled trial," *Archives of pediatrics & adolescent medicine*, vol. 161, no. 11, pp. 1075–1081, 2007.

[5] J. L. Pons, *Wearable robots: biomechatronic exoskeletons*. John Wiley & Sons, 2008.

[6] C. Thalman and P. Artemiadis, "A review of soft wearable robots that provide active assistance: Trends, common actuation methods, fabrication, and applications," *Wearable Technologies*, vol. 1, p. e3, 2020.

[7] M. A. Koch and J. M. Font-Llagunes, "Lower-limb exosuits for rehabilitation or assistance of human movement: A systematic review," *Applied Sciences*, vol. 11, no. 18, p. 8743, 2021.

[8] E. Bardi, M. Gandolla, F. Braghin, F. Resta, A. L. Pedrocchi, and E. Ambrosini, "Upper limb soft robotic wearable devices: a systematic review," *Journal of NeuroEngineering and Rehabilitation*, vol. 19, no. 1, pp. 1–17, 2022.

[9] N. Jarrassé and G. Morel, "Connecting a human limb to an exoskeleton," *IEEE Transactions on Robotics*, vol. 28, no. 3, pp. 697–709, 2011.

[10] J. Laut, M. Porfiri, and P. Raghavan, "The present and future of robotic technology in rehabilitation," *Current physical medicine and rehabilitation reports*, vol. 4, pp. 312–319, 2016.

[11] P. Kabir, M. Zareinejad, H. A. Talebi, M. Soleimanifar, M. Mavajian, and M. Ashoori, "Development and evaluation of a soft wearable knee rehabilitation apparatus," in *2022 10th RSI International Conference on Robotics and Mechatronics (ICRoM)*. IEEE, 2022, pp. 159–164.

[12] G. Aguirre-Ollinger, J. E. Colgate, M. A. Peshkin, and A. Goswami, "Design of an active one-degree-of-freedom lower-limb exoskeleton with inertia compensation," *The International Journal of Robotics Research*, vol. 30, no. 4, pp. 486–499, 2011.

[13] S. Sridar, P. H. Nguyen, M. Zhu, Q. P. Lam, and P. Polygerinos, "Development of a soft-inflatable exosuit for knee rehabilitation," in *2017 IEEE/RSJ International Conference on Intelligent Robots and Systems (IROS)*. IEEE, 2017, pp. 3722–3727.

[14] P. Polygerinos, N. Correll, S. A. Morin, B. Mosadegh, C. D. Onal, K. Petersen, M. Cianchetti, M. T. Tolley, and R. F. Shepherd, "Soft robotics: Review of fluid-driven intrinsically soft devices; manufacturing, sensing, control, and applications in human-robot interaction," *Advanced Engineering Materials*, vol. 19, no. 12, p. 1700016, 2017.

[15] F. Renda, M. Giorelli, M. Calisti, M. Cianchetti, and C. Laschi, "Dynamic model of a multibending soft robot arm driven by cables," *IEEE Transactions on Robotics*, vol. 30, no. 5, pp. 1109–1122, 2014.

[16] T. Abrar, F. Putzu, J. Konstantinova, and K. Althoefer, "Epam: Eversive pneumatic artificial muscle," in *2019 2nd IEEE International Conference on Soft Robotics (RoboSoft)*. IEEE, 2019, pp. 19–24.

[17] F. Aljaber, A. Hassan, T. Abrar, I. Vitanov, and K. Althoefer, "Soft inflatable fingers: An overview of design, prototyping and sensorisation for various applications," in *2023 IEEE International Conference on Soft Robotics (RoboSoft)*. IEEE, 2023, pp. 1–6.

[18] K. Althoefer, "Antagonistic actuation and stiffness control in soft inflatable robots," *Nature Reviews Materials*, vol. 3, no. 6, pp. 76–77, 2018.

[19] L. Cappello, K. C. Galloway, S. Sanan, D. A. Wagner, R. Granberry, S. Engelhardt, F. L. Haufe, J. D. Peisner, and C. J. Walsh, "Exploiting textile mechanical anisotropy for fabric-based pneumatic actuators," *Soft robotics*, vol. 5, no. 5, pp. 662–674, 2018.

[20] P. H. Nguyen and W. Zhang, "Design and computational modeling of fabric soft pneumatic actuators for wearable assistive devices," *Scientific reports*, vol. 10, no. 1, p. 9638, 2020.

[21] J. Nassour, F. H. Hamker, and G. Cheng, "High-performance perpendicularly-enfolded-textile actuators for soft wearable robots: Design and realization," *IEEE Transactions on Medical Robotics and Bionics*, vol. 2, no. 3, pp. 309–319, 2020.

[22] V. Sanchez, C. J. Walsh, and R. J. Wood, "Textile technology for soft robotic and autonomous garments," *Advanced functional materials*, vol. 31, no. 6, p. 2008278, 2021.

[23] C. Simpson, B. Huerta, S. Sketch, M. Lansberg, E. Hawkes, and A. Okamura, "Upper extremity exomuscle for shoulder abduction support," *IEEE Transactions on Medical Robotics and Bionics*, vol. 2, no. 3, pp. 474–484, 2020.

[24] Y. M. Zhou, C. Hohimer, T. Proietti, C. T. O'Neill, and C. J. Walsh, "Kinematics-based control of an inflatable soft wearable robot for assisting the shoulder of industrial workers," *IEEE Robotics and Automation Letters*, vol. 6, no. 2, pp. 2155–2162, 2021.

[25] L. Cappello, J. T. Meyer, K. C. Galloway, J. D. Peisner, R. Granberry, D. A. Wagner, S. Engelhardt, S. Paganoni, and C. J. Walsh, "Assisting hand function after spinal cord injury with a fabric-based soft robotic glove," *Journal of neuroengineering and rehabilitation*, vol. 15, no. 1, pp. 1–10, 2018.

[26] S. Sridar, Z. Qiao, N. Muthukrishnan, W. Zhang, and P. Polygerinos, "A soft-inflatable exosuit for knee rehabilitation: Assisting swing phase during walking," *Frontiers in Robotics and AI*, vol. 5, p. 44, 2018.

[27] J. Chung, R. Heimgartner, C. T. O'Neill, N. S. Phipps, and C. J. Walsh, "Exoboot, a soft inflatable robotic boot to assist ankle during walking: Design, characterization and preliminary tests," in *2018 7th ieee international conference on biomedical robotics and biomechatronics (biorob)*. IEEE, 2018, pp. 509–516.

[28] J. Realmuto and T. Sanger, "A robotic forearm orthosis using soft fabric-based helical actuators," in *2019 2nd IEEE International Conference on Soft Robotics (RoboSoft)*. IEEE, 2019, pp. 591–596.

[29] T. TolleyMichael, F. ShepherdRobert, C. GallowayKevin, J. WoodRobert, M. WhitesidesGeorge *et al.*, "A resilient, untethered soft robot," *Soft robotics*, 2014.

[30] D. Rus and M. T. Tolley, "Design, fabrication and control of soft robots," *Nature*, vol. 521, no. 7553, pp. 467–475, 2015.

[31] F. Putzu, T. Abrar, and K. Althoefer, "Plant-inspired soft pneumatic eversion robot," in *2018 7th IEEE International Conference on Biomedical Robotics and Biomechatronics (Biorob)*. IEEE, 2018, pp. 1327–1332.

[32] N. D. Naclerio and E. W. Hawkes, "Simple, low-hysteresis, foldable, fabric pneumatic artificial muscle," *IEEE Robotics and Automation Letters*, vol. 5, no. 2, pp. 3406–3413, 2020.

[33] H. Lipson, "Challenges and opportunities for design, simulation, and fabrication of soft robots," *Soft Robotics*, vol. 1, no. 1, pp. 21–27, 2014.

[34] O. Yasa, Y. Toshimitsu, M. Y. Michelis, L. S. Jones, M. Filippi, T. Buchner, and R. K. Katzschmann, "An overview of soft robotics," *Annual Review of Control, Robotics, and Autonomous Systems*, vol. 6, pp. 1–29, 2023.

[35] C.-P. Chou and B. Hannaford, "Measurement and modeling of mckibben pneumatic artificial muscles," *IEEE Transactions on robotics and automation*, vol. 12, no. 1, pp. 90–102, 1996.